First microsatellite markers for the pine catkin sawfly *Xyela concava* (Hymenoptera, Xyelidae) and their application in phylogeography and population genetics (#37530)

First revision

Guidance from your Editor

Please submit by **19 Sep 2019** for the benefit of the authors (and your $200 publishing discount).

Structure and Criteria
Please read the 'Structure and Criteria' page for general guidance.

Custom checks
Make sure you include the custom checks shown below, in your review.

Author notes
Have you read the author notes on the guidance page?

Raw data check
Review the raw data. Download from the materials page.

Image check
Check that figures and images have not been inappropriately manipulated.

Privacy reminder: If uploading an annotated PDF, remove identifiable information to remain anonymous.

Files

Download and review all files from the materials page.

1 Tracked changes manuscript(s)
1 Rebuttal letter(s)
3 Figure file(s)
9 Table file(s)

Custom checks

DNA data checks

- Have you checked the authors data deposition statement?
- Can you access the deposited data?
- Has the data been deposited correctly?
- Is the deposition information noted in the manuscript?

Structure your review

The review form is divided into 5 sections. Please consider these when composing your review:

1. **BASIC REPORTING**
2. **EXPERIMENTAL DESIGN**
3. **VALIDITY OF THE FINDINGS**
4. General comments
5. Confidential notes to the editor

You can also annotate this PDF and upload it as part of your review

When ready submit online.

Editorial Criteria

Use these criteria points to structure your review. The full detailed editorial criteria is on your guidance page.

BASIC REPORTING

- Clear, unambiguous, professional English language used throughout.
- Intro & background to show context. Literature well referenced & relevant.
- Structure conforms to PeerJ standards, discipline norm, or improved for clarity.
- Figures are relevant, high quality, well labelled & described.
- Raw data supplied (see PeerJ policy).

EXPERIMENTAL DESIGN

- Original primary research within Scope of the journal.
- Research question well defined, relevant & meaningful. It is stated how the research fills an identified knowledge gap.
- Rigorous investigation performed to a high technical & ethical standard.
- Methods described with sufficient detail & information to replicate.

VALIDITY OF THE FINDINGS

- Impact and novelty not assessed. Negative/inconclusive results accepted. *Meaningful* replication encouraged where rationale & benefit to literature is clearly stated.
- All underlying data have been provided; they are robust, statistically sound, & controlled.
- Speculation is welcome, but should be identified as such.
- Conclusions are well stated, linked to original research question & limited to supporting results.

Standout reviewing tips

The best reviewers use these techniques

Tip	*Example*
Support criticisms with evidence from the text or from other sources	*Smith et al (J of Methodology, 2005, V3, pp 123) have shown that the analysis you use in Lines 241-250 is not the most appropriate for this situation. Please explain why you used this method.*
Give specific suggestions on how to improve the manuscript	*Your introduction needs more detail. I suggest that you improve the description at lines 57- 86 to provide more justification for your study (specifically, you should expand upon the knowledge gap being filled).*
Comment on language and grammar issues	*The English language should be improved to ensure that an international audience can clearly understand your text. Some examples where the language could be improved include lines 23, 77, 121, 128 – the current phrasing makes comprehension difficult.*
Organize by importance of the issues, and number your points	*1. Your most important issue* *2. The next most important item* *3. …* *4. The least important points*
Please provide constructive criticism, and avoid personal opinions	*I thank you for providing the raw data, however your supplemental files need more descriptive metadata identifiers to be useful to future readers. Although your results are compelling, the data analysis should be improved in the following ways: AA, BB, CC*
Comment on strengths (as well as weaknesses) of the manuscript	*I commend the authors for their extensive data set, compiled over many years of detailed fieldwork. In addition, the manuscript is clearly written in professional, unambiguous language. If there is a weakness, it is in the statistical analysis (as I have noted above) which should be improved upon before Acceptance.*

First microsatellite markers for the pine catkin sawfly *Xyela concava* (Hymenoptera, Xyelidae) and their application in phylogeography and population genetics

Dustin Kulanek [Corresp., 1], **Stephan M Blank** [1], **Katja Kramp** [1]

[1] Senckenberg Deutsches Entomologisches Institut, Müncheberg, Germany

Corresponding Author: Dustin Kulanek
Email address: dustin.kulanek@senckenberg.de

Microsatellites are widely used as powerful markers in population genetics because of their ability to access recent genetic variation and to resolve subtle population genetic structures. However, their development, especially for non-model organisms with no available genome-wide sequence data, has been difficult and time-consuming. Here, a commercial high-throughput sequencing approach (HTS) was used for the very first identification of microsatellite motifs in the genome of *Xyela concava* and the design of primer pairs flanking those motifs. Sixteen of those primer pairs were selected and implemented successfully to answer questions on the phylogeography and population genetics of *X. concava*. The markers were characterized in three geographically distinct populations of *X. concava* and tested for cross-species amplification in two additional *Xyela* and one *Pleroneura* species (Xyelidae). All markers showed substantial polymorphism as well as revealing subtle genetic structures among the three genotyped populations. We also analyzed a fragment of the nuclear gene region of sodium/potassium-transporting ATPase subunit alpha (*NaK*) and a mitochondrial gene region partly coding for cytochrome oxidase subunit I (*COI*) to demonstrate different genetic resolutions and sex-biased patterns of these markers, and their potential for combined use in future studies on the phylogeography and population genetics of *X. concava.* Although a limited number of populations was analyzed, we already obtained new insights on the latter two topics. The microsatellites revealed a generally high gene flow between the populations, but also suggested a deep historical segregation into two genetic lineages. This deep genetic segregation was confirmed by *NaK*. While the high gene flow was unexpected, because of assumed restricted dispersal ability of *X. concava* and the discontinuous distribution of the host trees between the populations, the segregation of two lineages is comprehensible and could be explained by different refuge areas of the hosts during glacial times. The *COI* results showed a discordant strong genetic structure between all populations, which might be explained by the smaller effective population size of the mitochondrial genome.

However, given the frequent evidence of a similar nature in recent studies on sawflies, we also consider and discuss mitochondrial introgression on population level as an alternative explanation.

First microsatellite markers for the pine catkin sawfly *Xyela concava* (Hymenoptera, Xyelidae) and their application in phylogeography and population genetics

Dustin Kulanek[1], Stephan M. Blank[1], Katja Kramp[1]

[1]Senckenberg Deutsches Entomologisches Institut, Müncheberg, Germany

Corresponding Author:
Dustin Kulanek[1]
Eberswalder Str. 90, 15374 Müncheberg, Germany
Email address: Dustin.Kulanek@senckenberg.de

Abstract

Microsatellites are widely used as powerful markers in population genetics because of their ability to access recent genetic variation and to resolve subtle population genetic structures. However, their development, especially for non-model organisms with no available genome-wide sequence data, has been difficult and time-consuming. Here, a commercial high-throughput sequencing approach (HTS) was used for the very first identification of microsatellite motifs in the genome of *Xyela concava* and the design of primer pairs flanking those motifs. Sixteen of those primer pairs were selected and implemented successfully to answer questions on the phylogeography and population genetics of *X. concava*. The markers were characterized in three geographically distinct populations of *X. concava* and tested for cross-species amplification in two additional *Xyela* and one *Pleroneura* species (Xyelidae). All markers showed substantial polymorphism as well as revealing subtle genetic structures among the three genotyped populations. We also analyzed a fragment of the nuclear gene region of sodium/potassium-transporting ATPase subunit alpha (*NaK*) and a mitochondrial gene region partly coding for cytochrome oxidase subunit I (*COI*) to demonstrate different genetic resolutions and sex-biased patterns of these markers, and their potential for combined use in future studies on the phylogeography and population genetics of *X. concava.* Although a limited number of populations was analyzed, we ~~already~~ obtained new insights on the latter two topics. The microsatellites revealed a generally high gene flow between the populations, but also suggested a deep historical segregation into two genetic lineages. This deep genetic segregation was confirmed by *NaK*. While the high gene flow was unexpected, because of assumed restricted dispersal ability of *X. concava* and the discontinuous distribution of the host trees between the populations, the segregation of two lineages is comprehensible and could be explained by different ~~refuge~~ areas of the hosts during glacial times. The *COI* results showed a discordant strong genetic structure between all populations, which might be explained by the smaller effective population size of the mitochondrial genome. However, given the frequent evidence of a similar nature in recent studies on sawflies, we also consider and discuss mitochondrial introgression on population level as an alternative explanation.

Introduction

Xyelidae have always attracted the attention of taxonomists and systematists. They represent the sister group of the rest of the megadiverse insect order Hymenoptera (Ronquist et al., 2012; Klopfstein et al., 2013; Malm & Nyman, 2015), which is traditionally divided into the paraphyletic “Symphyta” (missing the wasp waist) and the monophyletic Apocrita (sharing a wasp waist as a derived feature) (Malm & Nyman, 2015). The recent inconsistent phylogenetic placement of xyelids together with Pamphiliidae and Tenthredinidae as sister clade to all remaining Hymenoptera by Peters et al. (2017) might have been caused by an artificial grouping due to shared very slow mutation rates in those groups (Ronquist et al., 2012).

The rich fossil record of Xyelidae includes the earliest fossil forms of Hymenoptera dating from the Middle–Upper Triassic (Kopylov, 2014). Proper knowledge of the phylogeography and

population genetics of xyelids is therefore important in understanding the underlying evolutionary processes, which in turn will help to understand the evolution of ~~the non-xyelid hymenopteran lineages~~. Unfortunately, such data are scarce for xyelids due to the rarity of many species, ephemerality of the imagines, and considerable problems in identifying species morphologically as well as genetically (e.g., Burdick 1961; Blank, Shinohara & Byun, 2005; Blank, Shinohara & Altenhofer, 2013; Blank et al., 2017; Blank & Kramp 2017). While a limited number of microsatellite studies has been conducted on sawflies (Hartel, Frederick & Shanower, 2003; Cook et al., 2011; Caron et al., 2013; Bittner et al., 2017), ~~non~~ has ~~been~~ focused on xyelids. Consequently, little is known about the population dynamics of this ~~ancestral species group~~, including effects of ephemerality of imagines and their dispersal ability, host adaption and host dependency, and reproduction mode.

Here, we report on the first developed and tested set of 16 polymorphic nuclear microsatellite markers for *Xyela concava* Burdick, 1961, to shed light on the latter issues. *X. concava* is widely distributed in southwestern USA, where it is closely associated with the pinyon-juniper woodland vegetation type of higher elevation semideserts, i.e., with pine species of the subgenus *Strobus* subsection *Cembroides* (Farjon 2010). Females oviposit into developing male cones of *Pinus cembroides*, *P. edulis* and *P. monophylla* (Fig. 1), where the larvae feed on the sporophylls. After having ceased feeding, *Xyela* larvae dig into the soil below the host trees and may diapause up to several years before pupating (Blank, Shinohara & Altenhofer, 2013). Imagines of the next generation emerge during spring and often visit flowering plants with easily accessible anthers, such as mountain mahogany (*Cercocarpus* spp.) and cliff-rose (*Purshia* spp.), from which they gather pollen for nutrition with their adapted mouthparts (Burdick 1961; Blank, personal observation). Flight behavior is described as erratic and slow (Burdick 1961). Therefore, given an assumed restricted dispersal ability and a close association with particular host species, it is intriguing to see how the variation within and among populations have been influenced by the distribution of the host trees during glacial and postglacial times. The high resolution power and therefore high capability of microsatellite markers to ~~access~~ subtle and recent population genetic structures makes them ~~very suitable for~~ this task. We used a commercial high-throughput sequencing approach for the development of the microsatellite markers and applied them to describe genetic structures and variation among and within three geographically distinct populations of *X. concava*. Furthermore, we compared the resolution of genetic variation of these markers with compiled data for one nuclear and one mitochondrial gene coding region and discuss their possible combined suitability for identifying genealogical lineages and answering phylogeographical questions. Finally, cross-amplification patterns for two species of *Xyela* and one of *Pleroneura*, sister taxon of *Xyela* (Smith 1967), are illustrated.

Material and methods

Sampling

Xyela larvae were extracted from staminate cones of pines as described by Blank, Shinohara & Altenhofer (2013) and stored in 100 % ethanol at -20 °C. We included in the analysis larvae originating from three collection sites which are located 900–1,200 km from each other (see Table S1). The specimens are preserved in the Senckenberg Deutsches Entomologisches Institut, Müncheberg, Germany. Since it is impossible to identify *Xyela* larvae to species level morphologically, they were *COI* barcoded and identified by comparison with sequences from imagines identified as *X. concava* morphologically (identification following Burdick (1961), reference sequences of imagines were published by Blank, Kramp & Shinohara (2017) and are deposited in the GenBank (NCBI) database, accession numbers KY198313 and KY198314). Finally, 98 larvae of *X. concava* were selected for the analysis (for detailed data see Table S1).

DNA extraction

Whole larvae were used for DNA extraction. The integument was slightly cut with a scalpel, so that the exterior stayed intact for later morphological inspection. DNA was extracted and purified with E.Z.N.A. Tissue DNA Kit (Omega Bio-Tek) according to the manufacturer's protocol, but with an extended 2 hour incubation time at 55 °C (Thermomixer, without shaking) for cell lysis. The extracted DNA was stored at -20 °C until later use. The integuments were retained and stored in 70 % ethanol.

Microsatellite marker development and screening

Total genomic DNA of a single female of *X. concava* (specimen ID: DEI-GISHym 30887, see Table S1) was extracted following the protocol described above. 10 ng/µl DNA in a total volume of 20 µl was sent to AllGenetics & Biology (Coruña, Spain) for the commercial identification of microsatellite motifs and the design of motif flanking primer pairs. A library was prepared for the DNA sample using the Nextera XTDNA kit (Illumina), following the manufacturer's instructions. The library was enriched with the following microsatellite motifs: AC, AG, ACG, and ATCT. Enriched DNA was sequenced in the Illumina MiSeq platform (PE300) and produced 3,043,190 paired-end reads. These paired-end reads were processed in Geneious 10.0.5 (Biomatters, Ltd.) using in-house developed scripts (property of AllGenetics & Biology) and overlapped into 1,521,595 sequences (trim error probability limit of 0.03). Primer design was carried out by AllGenetics & Biology in Primer 3 (Koressaar & Remm 2007; Untergrasser et al., 2012) for 500 sequences containing microsatellite motifs. For a preliminary screening, fifty primer pairs were picked and four *X. concava* larvae (DEI-GISHym 32824–32827) were used for tests of polymorphism. Furthermore, 12 specimens of *X. deserti* Burdick, 1961, 12 specimens of an undescribed *Xyela* species, possibly a member of the *X. alpigena* group (Blank & Kramp 2017), and six specimens of *Pleroneura koebelei* Rohwer, 1910 (see Table S1) were tested for cross-species amplification to check the marker system for potential use on two closely and one

more distantly related xyelid species. The PCR analysis included a temperature gradient in the primer annealing step to find the best conditions for each primer pair. PCR was carried out in a total volume of 5 µl containing 0.5 µl DNA, 0.1 µl of primers (10 pmol each) and 2.5 µl of 2x Multiplex PCR Plus Master mix (QIAGEN). The PCR protocol consisted of an initial DNA polymerase (HotStar Taq) activation step at 95 °C for 5 min, followed by 35 cycles of 30 s of 95 °C (DNA denaturation step), 90 s at 50 °C, 52 °C, 54 °C and 56 °C (primer annealing step, temperature ramp), and 30 s at 72 °C (elongation step); the last cycle was followed by a final 10 min extension step at 68 °C. 5 µl of the PCR product was visualized on a 2 % agarose gel. Primer pairs that produced no amplification, multiple or unexpected size PCR products were discarded. Eighteen primer pairs, showing discernably strong and specific signals, were picked for further analysis. 5'-end fluorescently labelled reverse primers (6-Fam (Biomers) and NED, VIC, PET (Thermo Fisher Scientific)) for the selected primer pairs were synthesized for multiplexing and capillary electrophoresis. PCR was carried out in four multiplex reactions for four *X. concava* DNA samples in a total volume of 10 µl containing 2.5 µl DNA, 1.0 µl of fluorescently labelled primer pair mix (0.5 pmol each, containing up to five primer pairs, depending on compatible annealing temperature, dye and expected fragment size range) and 5.0 µl of 2x Multiplex PCR Plus Master mix (QIAGEN). PCR reaction conditions were as described above with the respective optimal annealing temperature for each primer pair mix. Reactions were diluted 1:2 and sent to Macrogen Europe (Amsterdam, the Netherlands) for fragment analysis.

Allele sizes were scored using GeneMapper 5.0 (Applied Biosystems). No marker showed strong stutter peaks or intensive background signal. Two primer pairs appeared to be monomorphic and were excluded from further analyses. Sixteen primer pairs showed apparent polymorphism for the four tested samples and were finally selected (Table 1).

***COI* and *NaK* polymerase chain reaction analysis**

Primers used for amplification and sequencing are listed in Table 2. The mitochondrial region amplified is a 1,078 bp long fragment of cytochrome oxidase subunit I gene (*COI*). The first 658 bp of this fragment (from the 5' end) correspond to the standard barcode region of the animal kingdom (Hebert et al. 2004). Additionally, a 1,654 bp long fragment of the nuclear gene region of sodium/potassium-transporting ATPase subunit alpha (*NaK*) was amplified.

PCR reactions were carried out in a total volume of 20–25 µl containing 1.5–3.0 µl DNA, 1.2–2.5 µl of primers (5 pmol each) and 10.0–12.5 µl of 2x Multiplex PCR Plus Master mix (QIAGEN). The PCR protocol consisted of an initial DNA polymerase (HotStar Taq) activation step at 95 °C for 5 min, followed by 38–40 cycles of 30 s at 95 °C, 90 s at 49–59 °C depending on the primer set used, and 50–120 s (depending on the amplicon size) at 72 °C; the last cycle was followed by a final 30 min extension step at 68 °C. 3 µl of the PCR product was visualized on a 1.4 % agarose gel. Primers and dNTPs were inactivated with FastAP and Exonuclease I (Thermo Fisher Scientific). 1.7–2.2 U of both enzymes were added to 17–22 µl of PCR solution and incubated for 15 min at 37 °C, followed by 15 min at 85 °C. Purified PCR products were sent to Macrogen Europe (Amsterdam, the Netherlands) for sequencing. To obtain unequivocal

sequences, both sense and antisense strands were sequenced. Sequences were aligned manually with Geneious 11.0.5. Ambiguous positions (i.e., double peaks in chromatograms of both strands) due to heterozygosity or heteroplasmy were coded using IUPAC symbols. Sequences have been deposited in the GenBank (NCBI) database (accession numbers MK265017–MK265114 and MK264919–MK265016, for detailed data see Table S1).

Genetic data analysis

Estimations of genetic variation were obtained by calculating average number of alleles (N_A), observed (H_O) and expected heterozygosity (H_E) as well as deviations from Hardy-Weinberg equilibrium (HWE) for each locus for all *X. concava* populations using ARLEQUIN 3.5.2.2 (Excoffier & Lischer, 2010) and 1,000 permutations. The same program was used to assess the suitability of resolving population differentiation by estimating population pairwise measures of F_{ST} (1,000 permutations). The program GENEPOP 4.7.0 (Rousset, 2008) was used to estimate the inbreeding coefficient F_{IS} (1,000 permutations). GENEPOP was also used in combination with the ENA correction implemented in the program FreeNA (Chapuis & Estoup, 2007) to test for the presence and frequency of null alleles in the populations and to correct for the potential overestimation of F_{ST} values induced by the occurrence of null alleles (1,000 permutations). Number of genotypes (NG) in the dataset was counted with Excel. To test for isolation by distance, a Mantel test for the microsatellite data was performed (1,000 replicates) in ALLELES IN SPACE (Miller, 2005).

To assess the suitability of the microsatellite markers for ~~accessing~~ genetic population structures, three independent Bayesian assignment tests were carried out, one non-spatial using STRUCTURE 2.3.4 (Pritchard, Stephens & Donnelly, 2000) and two spatial model based using BAPS 6.0 (Corander, Waldmann & Sillanpää, 2003; Corander, Sirén & Arjas, 2008) and GENELAND 4.0.8 (Guillot, Mortier & Estoup, 2005). GENELAND assignment results for the microsatellite markers were also compared with results in GENELAND for the mitochondrial and nuclear gene coding markers (here without any comparison with a non-spatial assignment in STRUCTURE, since the model assumptions are likely to be violated for sequence data (Falush, Stephens & Pritchard, 2003)). In BAPS, a maximum number of 10 *K* was given as a prior. In STRUCTURE, ten replicates for each *K* from 1 to 10 were carried out with 50,000 burn-in steps followed by 100,000 MCMC. The online program STRUCTURE HARVESTER (Earl & vonHoldt, 2012) was used to infer the most likely value of *K*. GENELAND was carried out with an uncertainty on coordinates of 25 km, 100,000 iterations, a thinning to every 100 replicate and 10 independent runs. In STRUCTURE and GENELAND, a no admixture model and independency of allele frequency (uncorrelated model) was assumed, since correlated frequency models, though more powerful in detecting subtle differentiations, are more sensitive to departure from model assumptions (Guillot et al., 2012).

Results

The identification of microsatellite motifs ~~by~~ using HTS yielded 500 potential markers of which 50 were picked for a preliminary screening. Sixteen were finally implemented. Alongside primer pairs that produced no amplification or were monomorphic, some also ~~showed unexpected multiple size PCR products~~ and had to be discarded.

The microsatellite markers amplified 3–14 different alleles and 3–18 different genotypes per population and locus (Table 3). Observed heterozygosities ranged from 0.00 to 0.78 and were significantly lower than those expected under Hardy-Weinberg equilibrium except for one locus, indicating a deficiency of heterozygotes in the analyzed *Xyela concava* populations and/or the presence of null alleles. This deficit is also confirmed by positive F_{IS} values obtained for all but three loci in one population. Estimated frequencies of null alleles were variable depending on the respective microsatellite locus and *X. concava* population and varied between 0 and 39 % (Table 4).

The estimation of the frequency of null alleles, though highly variable depending on the locus-population combination, did not introduce any bias to our dataset and thus did not cause an overestimation of pairwise F_{ST} values.

The F_{ST} values uncorrected and corrected for the presence of null alleles showed higher values between the populations of Monitor Pass and Uinta Mountains as well as between the populations of Monitor Pass and Big Burro Mountains than the values between the populations of Uinta Mountains and Big Burro Mountains (Table 5). In general, all F_{ST} values were comparatively low (0.028–0.113) but either had a considerably narrow confidence interval or were significant or approaching the level of significance ($P = 0.055$). The F_{ST} values for *NaK* and *COI* were, in comparison, higher (0.215–0.740). While the values for *NaK* showed the same pattern as the microsatellite markers in respect of genetic relationship of the populations, the F_{ST} values for *COI* indicated relatively high differences between all populations (Table 6). The Mantel test showed no isolation by distance ($r^2 = 0.0173$, $P < 0.001$). While spatial assignment tests for *NaK* and the mircosatellites came up with the same pattern as the F_{ST} values ~~indicated by assigning two population~~ with high posterior probabilities to one genetic group or lineage (Figs. 2 and 3), the non-spatial STRUCTURE analysis for microsatellites was slightly non-confirmative, with genotypes from the Big Burro Mountains and Uinta Mountains assigned to one separate lineage, ~~but also~~ with genotypes from all three populations assigned to one shared overlapping genetic lineage. The analysis of the *COI* data revealed that each population represented one distinct cluster ($K = 3$) (Fig. 3B, C, D).

All microsatellite markers were successfully tested for cross-species amplification. For the three additional species of *Xyela* and *Pleroneura*, four markers showed polymorphic products and five were apparently monomorphic for *X. deserti* ~~Burdick, 1961~~. Eight markers showed polymorphic products for the new *Xyela* species of the *alpigena* group, while no or unspecific fragments were amplified for *Pleroneura koebelei* ~~Rohwer, 1910~~ (Table 7).

Discussion

Of 50 initial markers, only 16 could finally be implemented. Such high drop-out rates due to large numbers of repetitive motifs throughout the genome causing nonspecific binding of primers are already known (Schoebel et al., 2013). Other recent studies on invertebrates, using the same commercial HTS approach for the identification of SSR motifs, resulted in ~~between~~ 11 to 21 polymorphic microsatellite markers, which nonetheless could be applied successfully (Reineke et al., 2015; González-Castellano et al., 2018; Gomes et al., 2019).

The analyses demonstrated that the degree of variability of the new microsatellite marker set is adequate in that it reveals polymorphic alleles within and across populations. The low significant deviations from Hardy-Weinberg equilibrium as well as positive F_{IS} values for almost all loci in all populations could, however, have several causes. Given the ephemerality of the imagines and their fluctuating abundance due to extended diapausing, the major reason might have been a sampling bias, where only a fraction of each population was sampled (Wahlund effect). Furthermore, homozygote genotypes equally distributed across all populations indicated haploidy for altogether 26 specimens and may have had an impact on the discrepancy between the observed and expected heterozygosity. Thelytokous parthenogenesis – producing solely female offspring – which is known in xyelids (Blank, Shinohara & Altenhofer, 2013), also might have contributed to the deficiency. However, due to the observed genotypic variation across the data set, apomictic parthenogenesis seems unlikely (Caron et al., 2013).

The results based on the non-spatial model in STRUCTURE were not as confirmative as in the spatial-model based assignment tests. Since in STRUCTURE no spatial information and therefore fewer assumptions are incorporated, geographical barriers and distance as likely causes for differentiated populations might have been underestimated (Coulon et al., 2006). ~~Vice versa~~, because it does not include spatial information, STRUCTURE may here indicate a subtler genetic structure with possible higher exchange rates of the nuclear genome among all populations. However, both model applications told a broadly concordant narrative for the microsatellite markers, which are also supported by the low but significant F_{ST} values. First, the recent, seemingly discontinuous distribution of the hosts, *P. edulis* and *P. monophylla*, at higher elevations in mountain ranges with up to 100 km between single patches, apparently does not represent a barrier for recent and present gene flow. This is also supported by no isolation by distance ~~in the Mantel test~~. *X. concava* is assumed to be relatively stationary due to the observed slow and erratic flight behavior (Burdick, 1961). Therefore, other explanations for the ability to disperse over long distances should be considered, such as passive dispersal by wind.

Second, the proposed geographically remote and restricted refugia of the host species during glacial times (Bentancourt et al., 1991; Grayson 2011; Duran, Pardo & Mitton, 2012), and the considerably long distances between them, might have been ~~too much to overcome, and resulted in a very~~ restricted gene flow and ~~a~~ genetic segregation into two lineages. This assumption was also supported by the high and significant F_{ST} values and the genetic clustering of the *NaK* coding region, which due to the slower mutation rates presumably ~~rather displays~~ events in the past. In the F_{ST} statistics and assignment tests of the microsatellite data (displaying presumably

more recent events) the segregation could still be detected, but also a recent state of admixture was indicated. To test this hypothesis and a possibly ongoing admixture of the segregated lineages, populations of *X. concava* in hybrid zones and overlapping distribution areas of the host species should be included in future studies.

Compared to the results of the nuclear microsatellites and *NaK,* F_{ST} values and Bayesian statistics for the mitochondrial *COI* region showed a clear non-congruent pattern with a strong genetic structure among all three populations. One explanation could be the small effective population size (N_e) of the mitochondrial genome due to uniparental inheritance, which increases the rate at which populations will become genetically more structured (lineage sorting; Harrison, 1989). However, this non-congruent pattern also might have been caused by biased mitochondrial introgression as often found in "Symphyta" as recently discussed by Prous, Lee & Mutanen (2019, preprint). The authors assume that mitochondrial introgression in sawflies might be promoted by a combination of the haplodiploid reproduction system of Hymenoptera and the low mitochondrial mutation rates in sawflies. The assumption is partly based on theoretical models of Patten, Carioscia & Linnen (2015) showing that haplodiploid species are especially prone to biased mitochondrial introgression. Furthermore, Sloan, Havird & Sharbrough (2017) recently suggested that species with low mitochondrial mutation rates might favor a specific beneficial (possibly locally adapted and/ or novel) mitochondrial haplotype to compensate for deleterious mitonuclear mutation loads. The specific haplotype then selectively sweeps through a population (or species) and purges deleterious mitochondrial mutations (the alternative solution being compensatory co-evolutionary changes in the nuclear genome). Tendentially, this would lead to a strong mitochondrial population structure and a mitonuclear discordance, which might be reflected in the data set. Given the evidence for the very low evolutionary rates of molecular characters in xyelids (Ronquist et al., 2012), this might be especially true for them. Additionally, mitochondrial introgression might likely ~~to~~ be the cause for mitonuclear discordance in cases ~~in which~~ there is a general agreement among large numbers of nuclear loci but discordance with mitochondrial genealogies (Sloan, Havird & Sharbrough, 2017). Therefore, this new set of microsatellites may also be an attractive tool to indicate mitochondrial introgression at the population level of *X. concava* and other closely related xyelids.

Conclusions

The implemented new set of microsatellite markers will be valuable for future analyses of additional and less distantly located populations while unraveling the population structure of *Xyela concava*. Together with other nuclear gene coding markers it can be used to elucidate both old and recent divisions in the gene pool to reveal more details of the phylogeography of this species. Furthermore, especially because of different underlying evolutionary processes affecting the nuclear and mitochondrial genome, this new set of microsatellites can potentially be used to reveal processes such as mitochondrial introgression at population level.

Even from this small data set, some tentative phylogeographic trends can be stated for *X. concava*. This study covers only three populations but ~~already~~ indicates a segregation of two

genetic lineages and a recent state of admixture, which might have been caused by glacial retreat events. This would agree with proposed geographically separate glacial refugia of the host species. However, more populations covering the complete distribution ~~area~~ of *X. concava,* especially populations from overlapping distribution areas of the hosts, need to be analyzed to test this hypothesis.

Acknowledgements

We are grateful to C. Kutzscher (SDEI Müncheberg) for joining S.M. Blank during field work and for his support in the genetic lab. We thank A. Liston (SDEI Müncheberg) for a linguistic check of an earlier draft of the manuscript. We acknowledge the improvement of the manuscript by S.K. Monckton (~~Toronto~~) and an anonymous referee.

References

Aron S, de Menten L, Van Bockstaele DR, Blank SM, Roisin Y. 2005. When Hymenopteran Males Reinvented Diploidy. *Current Biology* 15:824–827.

Bittner TD, Hajek AE, Haavik L, Allison J, Nahrung H. 2017. Multiple introductions of *Sirex noctilio* (Hymenoptera: Siricidae) in northeastern North America based on microsatellite genotypes, and implications for biological control. *Biological Invasions* 19:1431–1447 DOI: 10.1007/s10530-016-1365-1.

Bentancourt JL, Schuster WS, Mitton JB, Anderson RS. 1991. Fossil and Genetic History of a Pinyon Pine (*Pinus edulis*). *Ecology* 72:1685–1697.

Blank SM, Kramp K. 2017. *Xyela davidsmithi* (Hymenoptera, Xyelidae), a new pine catkin sawfly with an unusual host association from the Sierra Nevada. *Proceedings of the Washington Entomological Society* 119:703–717.

Blank SM, Kramp K, Shinohara A. 2017. *Xyela fusca* spec. nov. from Japan elucidates East Asian–North American relationships of *Xyela* (Hymenoptera, Xyelidae). *Zootaxa* 4303:103–121 DOI: 10.11646/zootaxa.4303.1.6

Blank SM, Kramp K, Smith DR, Sundukov YN, Wei M, Shinohara A. 2017. Big and beautiful: The *Megaxyela* species (Hymenoptera, Xyelidae) of East Asia and North America. *European Journal of Taxonomy* 348:1–46 DOI: 10.5852/ejt.2017.348.

Blank SM, Shinohara A, Altenhofer E. 2013. The Eurasian species of *Xyela* (Hymenoptera, Xyelidae): Taxonomy, host plants and distribution. *Zootaxa* 3629:1–106 DOI: 10.11646/zootaxa.3629.1.1.

Blank SM, Shinohara A, Byun B-K. 2005. The East Asian *Xyela* species (Hymenoptera: Xyelidae) associated with Japanese Red Pine (*Pinus densiflora*; Pinaceae) and their distribution history. *Insect Systematics & Evolution* 36:259–278 DOI: 10.1163/187631205788838393.

Burdick DJ. 1961. A Taxonomic and Biological Study of the Genus *Xyela* Dalman in North America. *University of California Publications in Entomology* 17:285–356.

Caron V, Norgate M, Ede FJ, Nyman T, Sunnucks P. 2013. Novel microsatellite DNA markers indicate strict parthenogenesis and few genotypes in the invasive willow sawfly *Nematus oligospilus*. *Bulletin of Entomological Research* 103:74–88 DOI: 10.1017/S0007485312000429.

Chapuis MP, Estoup A. 2007. Microsatellite null alleles and estimation of population differentiation. *Molecular Biology and Evolution* 24:621–631 DOI: 10.1093/molbev/msl191.

Cook N, Aziz N, Hedley PE, Morris J, Milne L, Karley AJ, Hubbard SF, Russell JR. 2011. Transcriptome sequencing of an ecologically important graminivorous sawfly: a resource for marker development. *Conservation Genetics Resources* 3:789–795 DOI: 10.1007/s12686-011-9459-7.

Corander J, Sirén J, Arjas E. 2008. Bayesian spatial modeling of genetic population structure. *Computational Statistics* 23:111–129 DOI: 10.1007/s00180-007-0072-x.

Corander J, Waldmann P, Sillanpää MJ. 2003. Bayesian analysis of genetic differentiation between populations. *Genetics* 163:367–374 DOI: 10.1093/bioinformatics/bth250.

Coulon A, Guillot G, Cosson J-F, Angibault JMA, Aulagnier S, Cargnelutti B, Galan M, Hewison AJM. 2006. Genetic structure is influenced by landscape features: empirical evidence from a roe deer population. *Molecular Ecology* 15:1669–1679 DOI: 10.1111/j.1365-294X.2006.02861.x.

Duran KL, Pardo A, Mitton JB. 2012. From middens to molecules: Phylogeography of the piñon pine, *Pinus edulis*. *Journal of Biogeography* 39:1536–1544 DOI: 10.1111/j.1365-2699.2012.02704.x.

Earl DA, vonHoldt BM. 2012. STRUCTURE HARVESTER: a website and program for visualizing STRUCTURE output and implementing the Evanno method. *Conservation Genetics Resources* 4:359–361 DOI: 10.1007/s12686-011-9548-7.

Excoffier L, Lischer HEL. 2010. An Integrated Software Package for Population Genetics Data Analysis. *Molecular Ecology Resources* 10:564–567 DOI: 10.1111/j.1755-0998.2010.02847.x.

Funk DJ, Omland KE. 2003. Species-Level Paraphyly and Polyphyly: Frequency, Causes, and Consequences, with Insights from Animal Mitochondrial DNA. *Annual Review of Ecology, Evolution, and Systematics* 34:397–423. DOI: 10.1146/annurev.ecolsys.34.011802.132421.

Gomes SO, Souza IGB, Santos MF, Silva GR, Albrecht M, McKinley AS, Bentzen P, Diniz FM. 2019. Discovery of novel NGS-mined microsatellite markers and an exploratory analysis of genetic differentiation between two Western Atlantic populations of *Cardisoma guanhumi* Latreille, 1825 (Decapoda: Brachyura: Gecarcinidae). *Journal of Crustacean Biology* 39:181–185. DOI: 10.1093/jcbiol/ruy115.

González-Castellano I, Perina A, González-Tizón AM, Torrecilla Z, Martínez-Lage A. 2018. Isolation and characterization of 21 polymorphic microsatellite loci for the rockpool shrimp *Palaemon elegans* using Illumina MiSeq sequencing. *Scientific Reports* 8:8–13. DOI: 10.1038/s41598-018-35408-1.

Grayson DK. 2011. *The Great Basin: A Natural Prehistory*. Berkley and Los Angeles: University of California Press.

Guillot G, Mortier F, Estoup A. 2005. GENELAND: A computer package for landscape genetics. *Molecular Ecology Notes* 5:712–715 DOI: 10.1111/j.1471-8286.2005.01031.x.

Guillot G, Renaud S, Ledevin R, Michaux J, Claude J. 2012. A Unifying Model for the Analysis of Phenotypic, Genetic, and Geographic Data. *Systematic Biology* 61:897–911 DOI: 10.1093/sysbio/sys038.

Harrison RG. 1989. Animal mitochondrial DNA as a genetic marker in population and evolutionary biology. *Trends in Ecology and Evolution* 4:6–11. DOI: 10.1016/0169-5347(89)90006-2.

Hartel KD, Frederick BA, Shanower TG. 2003. Isolation and characterization of microsatellite loci in wheat stem sawfly *Cephus cinctus* and cross-species amplification in related species. *Molecular Ecology Notes* 3:85–87 DOI: 10.1046/j.1471-8286.

Hebert PDN, Penton EH, Burns JM, Janzen DH, Hallwachs W. 2004. Ten species in one: DNA barcoding reveals cryptic species in the neotropical skipper butterfly *Astraptes fulgerator*. *Proceedings of the National Academy of Sciences of the United States of America* 101:14812–14817. DOI: 10.1073/pnas.0406166101.

Klopfstein S, Vilhelmsen L, Heraty JM, Sharkey M, Ronquist F. 2013. The Hymenopteran Tree of Life: Evidence from Protein-Coding Genes and Objectively Aligned Ribosomal Data. *PLoS ONE* 8. DOI: 10.1371/journal.pone.0069344.

Kopylov DS. 2014. New sawflies of the subfamily Madygellinae (Hymenoptera, Xyelidae) from the Middle-Upper Triassic of Kyrgyzstan. *Paleontological Journal* 48:610–620 DOI: 10.1134/s0031030114060070.

Koressaar T, Remm M. 2007. Enhancements and modifications of primer design program Primer3. *Bioinformatics* 23:1289–1291. DOI: 10.1093/bioinformatics/btm091.

Malm T, Nyman T. 2015. Phylogeny of the symphytan grade of Hymenoptera: new pieces into the old jigsaw(fly) puzzle. *Cladistics* 31:1–17. DOI: 10.1111/cla.12069.

Miller MP. 2005. Alleles In Space (AIS): Computer software for the joint analysis of interindividual spatial and genetic information. *Journal of Heredity* 96:722–724. DOI: 10.1093/jhered/esi119.

Patten MM, Carioscia SA, Linnen CR. 2015. Biased introgression of mitochondrial and nuclear genes: A comparison of diploid and haplodiploid systems. *Molecular Ecology* 24:5200–5210. DOI: 10.1111/mec.13318.

Peters RS, Krogmann L, Mayer C, Donath A, Gunkel S, Meusemann K, Kozlov A, Podsiadlowski L, Petersen M, Lanfear R, Diez PA, Heraty J, Kjer KM, Klopfstein S, Meier R, Polidori C, Schmitt T, Liu S, Zhou X, Wappler T, Rust J, Misof B, Niehuis O. 2017. Evolutionary History of the Hymenoptera. *Current Biology* 27:1013–1018. DOI: 10.1016/j.cub.2017.01.027.

Pritchard JK, Stephens M, Donnelly P. 2000. Inference of population structure using multilocus genotype data. *Genetics* 155:945–959 DOI: 10.1111/j.1471-8286.2007.01758.x.

Prous M, Kramp K, Vikberg V, Liston A. 2017. North-Western Palaearctic species of *Pristiphora* (Hymenoptera, Tenthredinidae). *Journal of Hymenoptera Research* 59:1–190 DOI: 10.3897/jhr.59.12656.

Prous M, Lee KM, Mutanen M. 2019. Detection of cross-contamination and strong mitonuclear discordance in two species groups of sawfly genus *Empria*. *bioRxiv*. DOI: http://dx.doi.org/10.1101/525626.

Prous M, Vikberg V, Liston A, Kramp K. 2016. North-Western Palaearctic species of the

Pristiphora ruficornis group (Hymenoptera, Tenthredinidae). *Journal of Hymenoptera Research* 51:1–54 DOI: 10.3897/jhr.51.9162.

Reineke A, Assaf HA, Kulanek D, Mori N, Pozzebon A, Duso C. 2015. A novel set of microsatellite markers for the European Grapevine Moth *Lobesia botrana* isolated using next-generation sequencing and their utility for genetic characterization of populations from Europe and the Middle East. *Bulletin of Entomological Research* 105:408–416. DOI: 10.1017/S0007485315000267.

Ronquist F, Klopfstein S, Vilhelmsen L, Schulmeister S, Murray DL, Rasnitsyn AP. 2012. A Total-Evidence Approach to Dating with Fossils, Applied to the Early Radiation of the Hymenoptera. *Systematic Biology* 61:973–999 DOI: 10.1093/sysbio/sys058.

Rousset F. 2008. GENEPOP'007: A complete re-implementation of the GENEPOP software for Windows and Linux. *Molecular Ecology Resources* 8:103–106 DOI: 10.1111/j.1471-8286.2007.01931.x.

Schoebel CN, Brodbeck S, Buehler D, Cornejo C, Gajurel J, Hartikainen H, Keller D, Leys M, Říčanová Š, Segelbacher G, Werth S, Csencsics D. 2013. Lessons learned from microsatellite development for nonmodel organisms using 454 pyrosequencing. *Journal of Evolutionary Biology* 26:600–611. DOI: 10.1111/jeb.12077.

Sloan DB, Havird JC, Sharbrough J. 2017. The on-again, off-again relationship between mitochondrial genomes and species boundaries. *Molecular Ecology* 26:2212–2236. DOI: 10.1111/mec.13959.

Smith DR. 1967. A review of the larvae of Xyelidae, with notes on the family classification (Hymenoptera). *Annals of the Entomological Society of America* 60:376–384. DOI: 10.1093/aesa/60.2.376.

Untergasser A, Cutcutache I, Koressaar T, Ye J, Faircloth BC, Remm M, Rozen SG. 2012. Primer3 – new capabilities and interfaces. *Nucleic Acids Research* 40:1–12. DOI: 10.1093/nar/gks596.

Table 1 (on next page)

Sixteen polymorphic microsatellite loci and the corresponding flanking primer pairs identified in the pine catkin sawfly *Xyela concava*

Locus	Size range (bp)	Motif	Ta in °C	label	Primer sequence (5'─3')
AG_30887_445	75–93	$AAG_{(11)}$	50	VIC	F: GTCTCGACTCCCTCCTACGA R: ACGGAAGTGCATCGGATCTTC
AG_30887_046	195–225	$AGC_{(30)}$	50	PET	F: CCTTTCGTCCTGGTTGACCA R: GATACGCCAGCCTATCCGTC
AG_30887_083	178–190	$AAG_{(10)}$	50	6-Fam	F: TTCCAGTTTCTTGCAACGCG R: ATTCGCAAGCCTCTTCTGCA
AG_30887_188	179–188	$AAT_{(9)}$	50	NED	F: GCGGCGGTATAATGAGTCGT R: GGAAAGTGACTGCTACCGGT
AG_30887_479	93–102	$ACT_{(8)}$	50	PET	F: GCTGTTCACATGGCAGGTAG R: CCACCATCCCTACTACGGCT
AG_30887_193	110–134	$AGC_{(17)}$	50	VIC	F: AGAGTGCCAACGTGGGAAAT R: TTACTTTGCCCATGCCATGC
AG_30887_234	376–424	$AATGCG_{(8)}$	50	PET	F: AGTCTGATCCTTCCTGCGGA R: ATACGTGCCAGTTCGATCGT
AG_30887_282	239–263	$AGC_{(10)}$	50	6-Fam	F: CTGTGCCTACGTCCCTTAGG R: CCCATCGTTTGGTCGGTAGA
AG_30887_286	103–121	$AGC_{(8)}$	50	NED	F: GCGTCCGTCTGAAATCTTGG R: CATTCGCATTCGACGCACTC
AG_30887_179	111–126	$AGC_{(9)}$	50	6-Fam	F: CCCGTTCGTAAATCGGTCCT R: GACGTGGAATCGGTGGACTC
AG_30887_460	90–116	$AT_{(5)}$	50	PET	F: ACGTACTTATTGGGCGCGAA R: TTTACATGCTGTACACCGGGA
AG_30887_347	237–249	$AAG_{(8)}$	50	PET	F: CCCGGACCTCGTGCTATTC R: GGCGACAATCCCACGTGATA
AG_30887_393	136–175	$AAG_{(8)}$	50	6-Fam	F: CCATCACTGTGCCGCGATAT R: GCACCTCAGGGATCCTCAAT
AG_30887_414	122–179	$AAG_{(8)}$	50	NED	F: TGATTTGTGCAACCGAGGGA R: CCCTTTATTCTCAGCAACCGC
AG_30887_012	130–148	$AGG_{(9)}$	50	PET	F: TTCCGGACGACTTTGACCTG R: CCTCGATTCCGATTCCCGTT
AG_30887_223	120–186	$AAG_{(9)}$	50	6-Fam	F: TCAAAGCGGAGAAAGAGCGT R: TTAACCGCCATCGACCGTTC

1

Table 2 (on next page)

Nuclear *NaK* and mitochondrial *COI* primers used for amplification (PCR) and sequencing (seq)

Gene Region	Primer name	Primer sequence (5'-3')	Ta in °C	PCR/ Sequencing	Reference
COI	symF1	TTTCAACWAATCATAAARAYATTGG	49	PCR, seq	Prous et al. 2016
COI	symR1	TAAACTTCWGGRTGICCAAARAATC	49	PCR/ seq	Prous et al. 2016
COI	symC1-J1751	GGAGCNCCTGATATAGCWTTYCC	49	seq	Prous et al. 2016
NaK	NaK263F	CTYAGCCAYGCRAARGCRAARGA	59	PCR/ seq	Prous et al. 2017
NaK	NaK907Ri	TGRATRAARTGRTGRATYTCYTTIGC	59	seq	Prous et al. 2017
NaK	NaK1250Fi	ATGTGGTTYGAYAAYCARATYATIGA	59	seq	Prous et al. 2017
NaK	NaK1918R	GATTTGGCAATNGCTTTGGCAGTDAT	59	PCR/ seq	Prous et al. 2017

Table 3 (on next page)

Comparative genetic diversity values for the three *Xyela concava* populations

Analyzed for each of the 16 microsatellite loci and on average over all loci including number of alleles (N_A), Number of genotypes (NG), observed (H_O) and expected (H_E) heterozygosity and estimates of F_{IS}

Locus	Big Burro Mountains				Monitor Pass				Uinta Mountains			
	N_A/NG	F_{IS}	H_O	H_E	N_A/NG	F_{IS}	H_O	H_E	N_A/NG	F_{IS}	H_O	H_E
AG_30887_445	6/7	0.91	0.07	0.78*	6/11	0.50	0.40	0.79*	7/12	0.43	0.40	0.69*
AG_30887_046	10/11	0.33	0.61	0.85*	9/14	0.44	0.47	0.82*	7/11	0.04	0.78	0.80*
AG_30887_083	5/7	0.39	0.43	0.69*	3/5	0.63	0.20	0.53*	4/5	-0.18	0.63	0.53*
AG_30887_188	4/6	0.84	0.11	0.66*	3/5	0.31	0.37	0.53*	3/5	0.63	0.25	0.66*
AG_30887_479	3/4	0.22	0.43	0.54*	4/5	0.79	0.10	0.47*	4/6	-0.06	0.53	0.49*
AG_30887_193	6/8	0.31	0.50	0.72*	5/12	0.47	0.40	0.74*	7/13	0.04	0.78	0.80*
AG_30887_234	6/9	0.34	0.50	0.75*	6/8	0.42	0.40	0.68*	6/9	0.21	0.63	0.78*
AG_30887_282	8/8	0.40	0.46	0.77*	6/9	0.61	0.30	0.75*	6/9	-0.03	0.73	0.70*
AG_30887_286	6/8	0.76	0.18	0.74*	5/9	0.24	0.47	0.61	7/11	0.53	0.35	0.74*
AG_30887_179	3/3	1.00	0.00	0.62*	5/7	0.55	0.20	0.43*	5/6	0.76	0.15	0.61*
AG_30887_460	6/6	0.75	0.14	0.55*	4/4	0.30	0.13	0.18*	6/6	0.74	0.15	0.56*
AG_30887_347	4/5	0.34	0.43	0.64*	3/6	0.51	0.33	0.67*	4/7	0.06	0.63	0.66*
AG_30887_393	7/7	0.82	0.11	0.59*	6/10	0.44	0.40	0.71*	5/9	0.67	0.20	0.59*
AG_30887_414	12/12	0.35	0.54	0.82*	10/18	0.54	0.40	0.86*	9/13	0.13	0.68	0.77*
AG_30887_012	5/7	0.90	0.07	0.73*	3/4	0.51	0.27	0.54*	3/4	0.67	0.23	0.67*
AG_30887_223	9/11	0.76	0.14	0.80*	14/18	0.36	0.47	0.89*	13/15	0.72	0.23	0.82*
Mean		0.59	0.29	0.71		0.48	0.33	0.64		0.33	0.46	0.68
S.D.		0.26	0.21	0.09		0.13	0.12	0.18		0.33	0.24	0.10

* significant departure from H-W equilibrium ($P < 0.05$)

S.D. = standard deviation

4

Table 4(on next page)

Estimated null allele frequencies for each of the 16 polymorphic microsatellite loci and each population including the average null allele frequency

Estimated null allele frequency

Locus	Big Burro Mts	Monitor Pass	Uinta Mts
AG_30887_445	0.395	0.221	0.167
AG_30887_046	0.165	0.191	0.028
AG_30887_083	0.175	0.229	0.041
AG_30887_188	0.334	0.116	0.247
AG_30887_479	0.095	0.267	0.040
AG_30887_193	0.130	0.194	0.037
AG_30887_234	0.161	0.184	0.087
AG_30887_282	0.194	0.260	0.036
AG_30887_286	0.314	0.073	0.208
AG_30887_179	0.381	0.190	0.282
AG_30887_460	0.259	0.000	0.257
AG_30887_347	0.148	0.200	0.048
AG_30887_393	0.309	0.163	0.247
AG_30887_414	0.196	0.245	0.053
AG_30887_012	0.378	0.183	0.264
AG_30887_223	0.319	0.162	0.314
Mean	0.247	0.180	0.147

Table 5 (on next page)

Pairwise F_{ST} estimates between populations of *Xyela concava* for the 16 microsatellite loci including corresponding *P* values and confidence intervals

Estimates are given both uncorrected and corrected for the presence of null alleles. Bold typeface denotes pairwise F_{ST} estimates that are significantly different from zero ($P < 0.005$). Values in square brackets indicate 95 % confidence intervals for pairwise corrected F_{ST} estimates

F_{ST} uncorrected	Big Burro Mts	Monitor Pass	Uinta Mts
Big Burro Mts	*		
Monitor Pass	**0.09182**	*	
Uinta Mts	0.02254	**0.07705**	*

F_{ST} ENA corrected	Big Burro Mts	Monitor Pass	Uinta Mts
Big Burro Mts	*		
Monitor Pass	0.083 [0.054, 0.115]	*	
Uinta Mts	0.015 [0.004, 0.028]	0.065 [0.041, 0.094]	*

Table 6 (on next page)

Pairwise F_{ST} estimates between populations of *Xyela concava* for *NaK* and *COI* including corresponding *P* values

Bold typeface denotes pairwise F_{ST} estimates that are significantly different from zero ($P < 0.005$)

NaK	BB Mts	Mon Pass	Uinta Mts
Big Burro Mts	*		
Monitor Pass	**0.740**	*	
Uinta Mts	**0.215**	**0.680**	*
COI	BB Mts	Mon Pass	Uinta Mts
Big Burro Mts	*		
Monitor Pass	**0.699**	*	
Uinta Mts	**0.508**	**0.678**	*

Table 7 (on next page)

Cross-species amplification

(-) no product, (+) monomorphic product, (++) polymorphic product

Locus	*Xyela deserti*	*Xyela* spec. nov.	*Pleroneura koebelei*
AG_30887_445	-	-	-
AG_30887_046	+	++	-
AG_30887_083	-	-	-
AG_30887_188	-	-	-
AG_30887_479	+	++	-
AG_30887_193	-	++	-
AG_30887_234	+	++	-
AG_30887_282	++	++	-
AG_30887_286	++	++	-
AG_30887_179	-	-	-
AG_30887_460	-	-	-
AG_30887_347	++	++	-
AG_30887_393	+	-	-
AG_30887_414	++	-	-
AG_30887_012	-	-	-
AG_30887_223	+	++	-

Figure 1

Location of the collection areas and distribution of the host species

[p]Credit *Pinus spec*. shape files: https://data.usgs.gov/metadata[p]

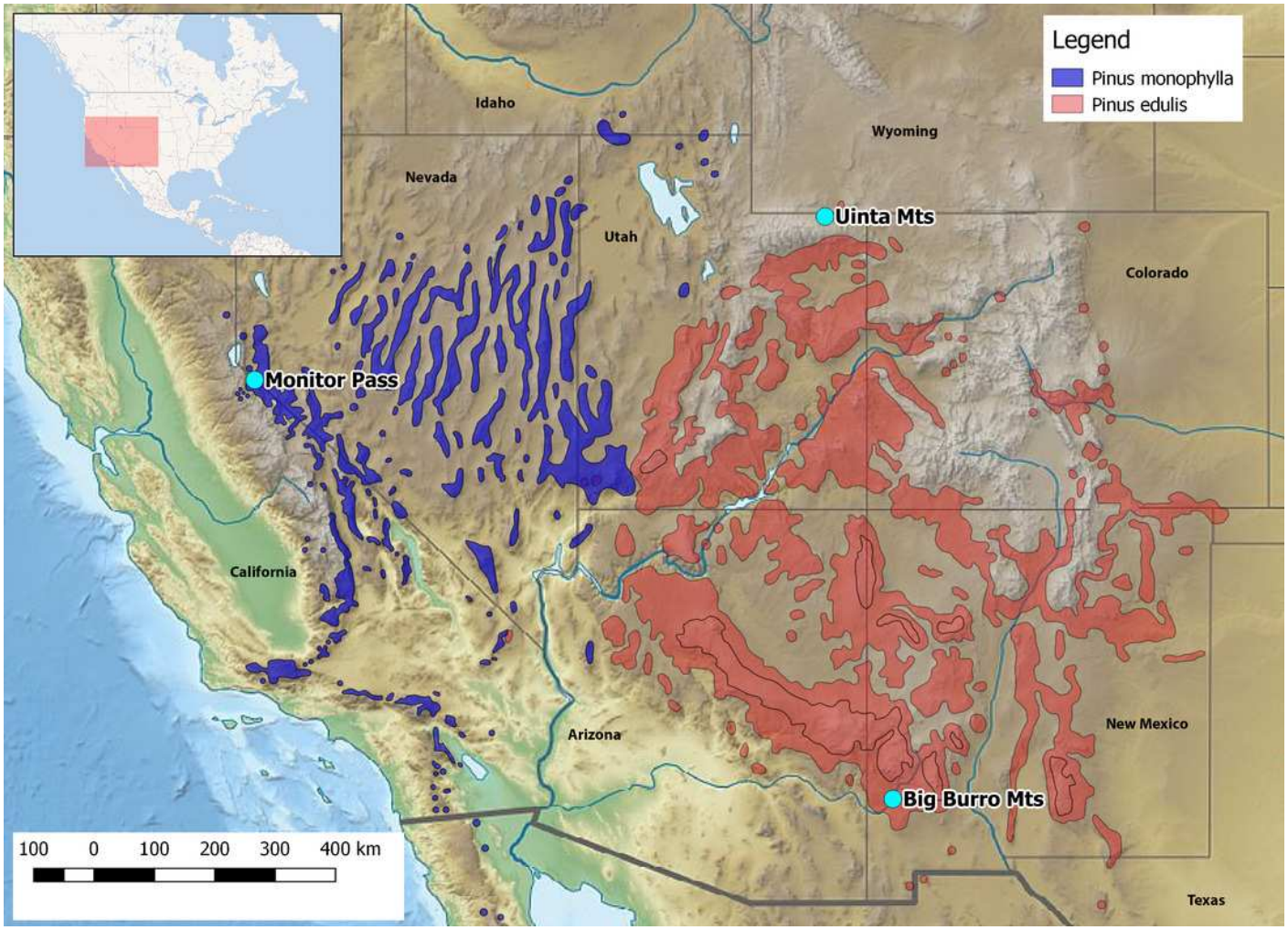

Figure 2

Bayesian assignment of *Xyela concava* populations to each of the identified clusters (*K* = 2) for the microsatellite markers

(A) GENELAND (Posterior probabilities are indicated in the scale bar. The contour lines in the maps indicate the spatial positions of genetic discontinuities. Lighter shading indicates a higher probability of belonging to the genetic population), (B) BAPS (the area of each population is proportional to the number of specimens used) and (C) STRUCTURE

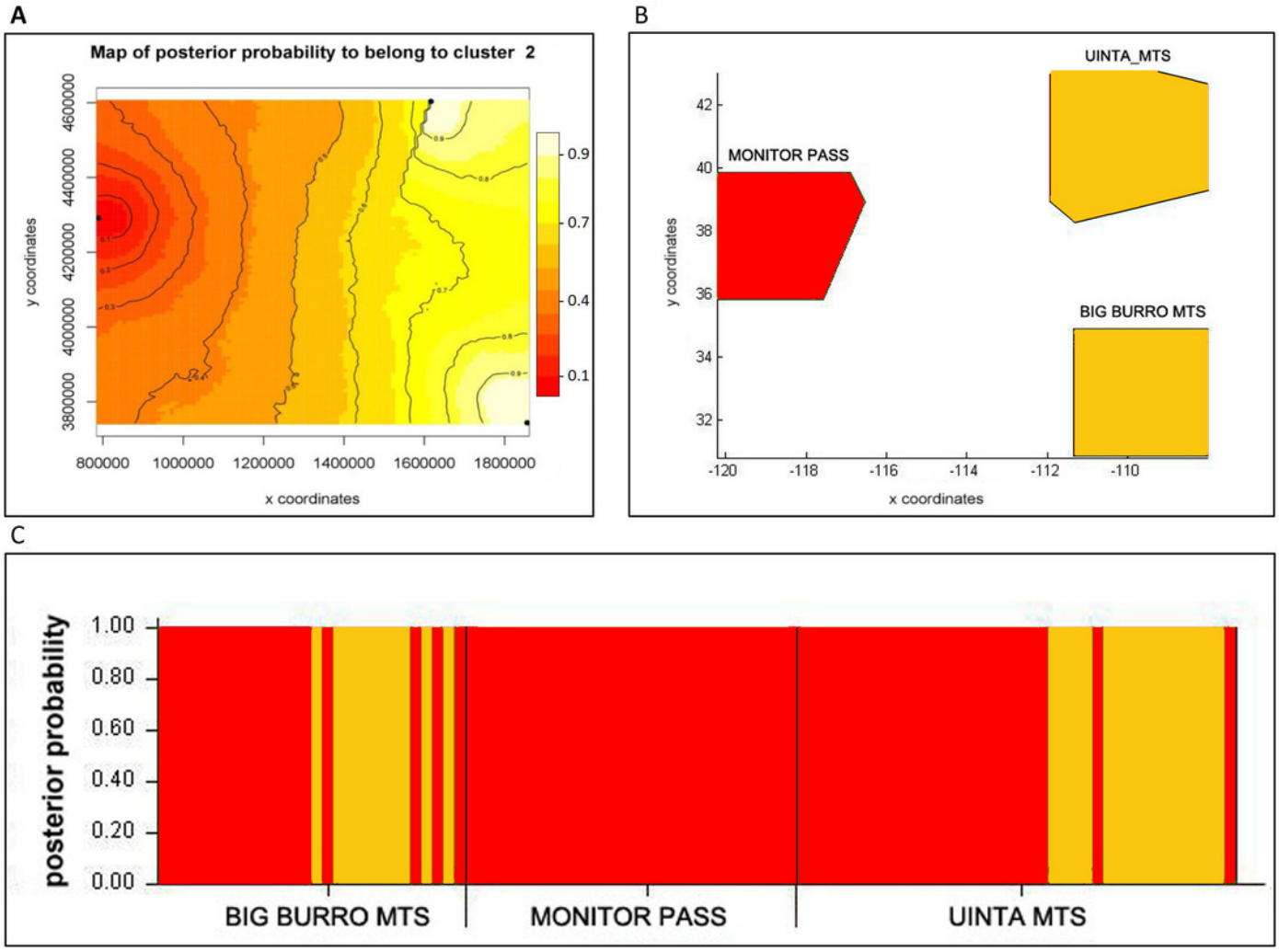

Figure 3

Bayesian spatial assignment (GENELAND) of *Xyela concava* populations to each of the identified clusters for (A) *NaK* (*K* = 2) and (B), (C), (D) *COI* (*K* = 3).

The different colors represent the estimated posterior probabilities of the membership to each cluster. Posterior probabilities are indicated in the scale bar. The contour lines in the maps indicate the spatial positions of genetic discontinuities. Lighter shading indicates a higher probability of belonging to the genetic population.

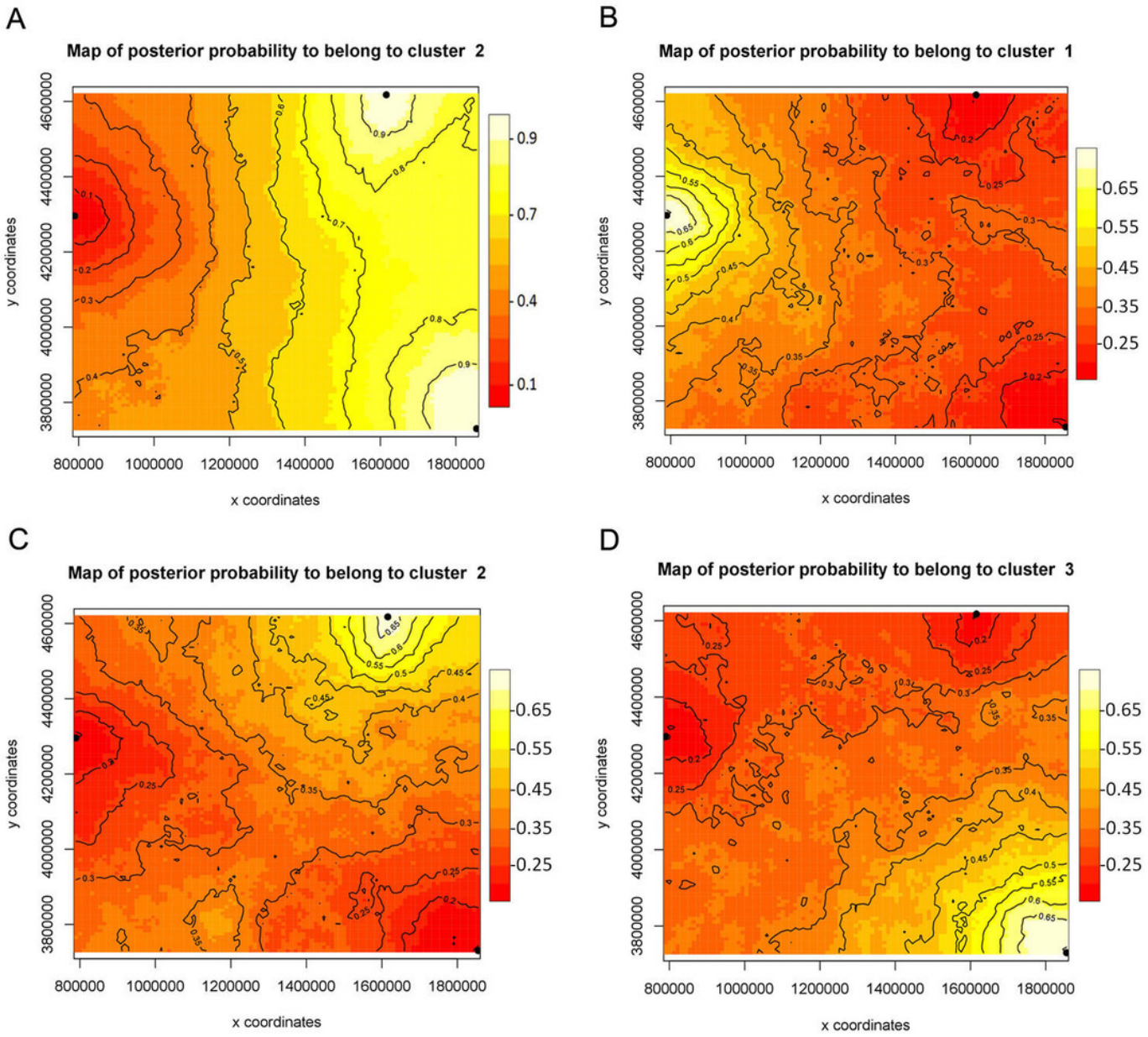
A
Map of posterior probability to belong to cluster 2
y coordinates
x coordinates
B
Map of posterior probability to belong to cluster 1
y coordinates
x coordinates
C
Map of posterior probability to belong to cluster 2
y coordinates
x coordinates
D
Map of posterior probability to belong to cluster 3
y coordinates
x coordinates